






# MACHINE LEARNING METHODS AS APPLIED TO MODELLING THERMAL CONDUCTIVITY OF EPOXY-BASED COMPOSITES WITH DIFFERENT FILLERS FOR AIRCRAFT

Oleh YASNIY , Mykola MYTNYK , Pavlo MARUSCHAK ✉, Andriy MYKYTYSHYN , Iryna DIDYCH 

*Ternopil Ivan Puluj National Technical University, Ruska str. 56, 46001 Ternopil, Ukraine*

## Article History:

- received 19 November 2023
- accepted 24 January 2024

**Abstract.** The thermal conductivity coefficient of epoxy composites for aircraft, which are reinforced with glass fiber and filled with aerosil,  $\gamma$ -aminopropyl-aerosil, aluminum oxide, chromium oxide, respectively, was simulated. To this end, various machine learning methods were used, in particular, neural networks and boosted trees. The results obtained were found to be in good agreement with the experimental data. In particular, the correlation coefficient in the test sample was 0.99%. The prediction error of neural networks in the test samples was 0.5; 0.3; 0.2%, while that of boosted trees was 1.5; 0.9%.

**Keywords:** epoxy-based composites, fillers, modelling, aircraft, aerospace applications, machine learning.

✉Corresponding author. E-mail: [maruschak.tu.edu@gmail.com](mailto:maruschak.tu.edu@gmail.com)

## 1. Introduction

In the aircraft design, the fuselage, wings, tail unit, engine nacelle, and interior parts can be made from composite materials. It is urgent to develop new materials, innovative solutions for technology and production equipment, allowing for high strength and aerodynamic characteristics with economic efficiency in aircraft production conditions.

An increasingly growing automation of technology along with numerous data sets account for the need in machine learning methods, which, instead of being programmed, are capable of analyzing data and learning from them (Konovalenko et al., 2021). In the presence of experimental data, machine learning algorithms are known to solve the problems of fracture mechanics with great accuracy. In particular, they are capable of predicting the life of a fatigue crack that occurred in an aluminum alloy using a neural network (Mohanty et al., 2009) and fatigue fracture diagrams of aluminum alloy D16T subjected to the regular loading conditions with the load cycle asymmetry  $R = 0; 0.2; 0.4; 0.6$  (Yasnii et al., 2018). The authors (Zhang & Wei, 2022) predicted the propagation of a fatigue crack under conditions of variable amplitude loading by means of Lagrange interpolation based on an artificial neural network. In addition, the stress-strain diagrams of aluminum alloy AMg6 (Yasniy et al., 2020; 2022a) and AL-6061 (Yasniy et al., 2022b) were simulated using machine learning methods. Neural networks have also aided

the authors (Bezerra et al., 2007) in predicting the stress-strain diagrams that describe the shear of such composites as carbon fiber/epoxy resin and glass fiber/epoxy resin. While the bending properties of 3D-printed carbon/epoxy composites with different processing parameters were predicted by the authors (Monticeli et al., 2022) using an artificial neural network and statistical methods. In Stephen et al. (2022), the impact characteristics of fiber-reinforced polymer composites are modeled using the finite element method and an artificial neural network. In particular, a multi-scale approach based on the stochastic integrated machine training was used in Liu et al. (2022) in order to predict the thermal conductivity of polymer composites reinforced with carbon nanotubes. Therefore, different machine training methods appear relevant when it comes to predicting the thermal conductivity coefficient of polymer composites.

In general, polymer composite materials are often used in the production of load-bearing structures, such as equipment for gas mains, radio engineering products, and aircraft structures because of their superior physical-mechanical and thermo-physical properties (Stukhlyak et al., 2015; Dobrotvor et al., 2021). The issues related to the preferable filler type, the degree of filling and dispersion, and the polymerization conditions of the filled composition are considered while creating composite materials. In particular, composites with improved technological and service characteristics ensure a strong and stable bond

between the surfaces of the filler and the polymer. The thermal expansion of polymers is characterized by certain features in the range of glass transition temperature. These features are known to depend on the temperature variation rate. Therefore, investigations into the thermophysical properties that affect the service characteristics remain topical.

This research aims at predicting the thermal conductivity coefficient of the epoxy composites reinforced with glass fiber and filled with aerosil,  $\gamma$ -aminopropylaerosil, aluminum oxide, chromium oxide, respectively, during their heating. For this purpose, various machine learning methods are used, in particular, neural networks and boosted decision trees. The results obtained are compared.

## 2. Materials and methods

### 2.1. Thermophysical research of filled epoxy composites

Epoxy composites with enhanced service properties can be obtained subject to optimizing their production technology and the process of filling the matrix with the fillers of different chemical nature, composition and size, which are characterized by the improved mechanical and thermophysical properties. A small amount of fillers introduced into the epoxy matrix, the former being chemically active in relation to the matrix (1 wt % of aerosil and 1 wt % of  $\gamma$ -aminopropylaerosil per 100 wt %s), entails a significant increase in  $\lambda$ . This is associated with a strong bond formed by the chemical and chemisorption interaction between the binder macromolecules and the aerosil surface. At the same time, a large amount of aerosil introduced into the epoxy matrix causes a decreased thermal conductivity of the material, which is due to an increased length of the separation boundary and a weakened interaction of OH groups between the filler and the binder.

A low concentration of  $\text{Al}_2\text{O}_3$  (up to 30 wt %) introduced into the binder causes little change in the thermal conductivity coefficient of the epoxy composite, as compared to the thermal conductivity of the unfilled binder. Epoxy composites with the  $\text{Al}_2\text{O}_3$  content in the matrix exceeding 30 wt % are characterized by an increased thermal conductivity compared to the unfilled binder. This is because the thermal conductivity of the filler itself affects the thermal conductivity of the material as a whole. In such composites, there is no bond between the matrix and the filler.

The mechanisms characteristic of both chemically active ( $\gamma$ -aminopropylaerosil and aerosil) and inactive (aluminum oxide) fillers are also inherent in the epoxy composite filled with chromium oxide. Therefore, for this filler, the thermal conductivity coefficient is determined by the competing contribution made by the mechanisms that account for its change as described above. In one case, physical nodes formed between the matrix and the active centers on the surface of the filler particles lead to an increase in  $\lambda$ . This normally occurs at low temperatures due to the additional hydrogen bonds formed at the phase bound-

ary. In the other case, it leads to a decrease in  $\lambda$  due to a higher defectiveness of the boundary layer. In addition, thermal resistance also increases in response to the elevated temperature caused by failure of physical nodes. At the same time, the thermal conductivity of the filler accounts for an increase in the filler content with an increase in the thermal conductivity of the matrix.

In general, the thermophysical properties of epoxy composite materials depend both on the nature and amount of the filler and the specifics of the particle surface. In addition, these characteristics can be improved by introducing the fillers that are chemically active in relation to the matrix. These fillers form a strong bond between the binder macromolecules and the filler surface, which occurs as a result of the chemical and chemisorption interaction.

### 2.2. Methods of machine learning

The most common model of a neural network is a multi-layer perceptron, in which neurons are arranged in layers from input to output (Haykin, 2006). The structure of a three-layer neural network is shown in Figure 1. In particular, the concentration of the mass fraction  $C$  in the filler and the temperature  $T$  serve as input parameters, while the thermal conductivity coefficient  $\lambda$  is the output parameter. Accordingly,  $w_{ij}$  and  $w_{jk}$  are the synaptic weights between different layers of the network, and  $(H_1, H_2, \dots, H_n)$  are the thresholds of the hidden layer.

The input signal passes to the neurons of the hidden layer, while the output signals of the hidden layer of the neural network are the inputs of the next one. Neurons of each layer are the output signals of only the previous one.

To attain the best neural network architecture, a number of numerical experiments were conducted using the "input-output" pairs and different activation functions, such as tangential, logarithmic ones and others, thus varying the number of neurons in the hidden layer. In the process of learning, the network uses error backpropagation algorithms, that is, it adjusts its weights to minimize the error between the predicted and experimental data.

The network operation algorithm is based on Haykin (2006) the following Equations:

$$NET_{jl} = \sum_m w_{mjl} \times x_{mjl}; \quad (1)$$

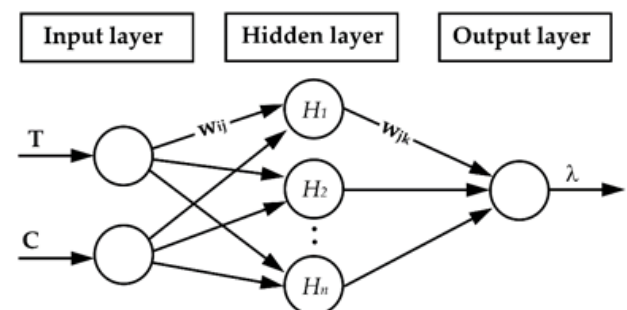


**Figure 1.** A three-layer neural network architecture with one hidden layer and one output layer

$$OUT_{jl} = F(NET_{jl} - \theta_{jl}); \quad (2)$$

$$x_{mj(l+1)} = OUT_{ml}, \quad (3)$$

where  $i$  is the number of entry into the layer;  $j$  is the neuron number in the layer;  $l$  is the layer number;  $x_{ijl}$  is the  $i$ -th input signal of the  $j$ -th neuron in layer  $l$ ;  $w_{ijl}$  is the weight coefficient of the  $i$ -th input of the  $j$ -th neuron of layer  $l$ ;  $NET_{jl}$  is the NET signal of the  $j$ -th neuron of layer  $l$ ;  $Out_{jl}$  is the output signal;  $F$  is the nonlinear activation function;  $\theta_{jl}$  is the threshold level of a particular neuron.

The choice of the neural network architecture, learning algorithm, error function, and activation function of the hidden and output layers is important when building a network. In addition, the stopping parameter of the neural network learning was the number of epochs, which in this research was equal to 1000.

The algorithm of boosted trees is a powerful method of the intelligent data analysis (Alpayndin, 2010). It is commonly used to predict data and in situations when the results of one decision affect those of the subsequent one, that is, in order to make sequential decisions. The model structure is tree-like (Figure 2). In general, a boosted tree consists of internal nodes and leaves that are added during learning depending on the problem complexity. In particular, ovals are the decision nodes, while rectangles are the leaf nodes. The univariate decision node splits along one axis, and successive splits are orthogonal to each other. After the first split,  $\{x|x_1 < w_{10}\}$  is pure and is not split further.

The major advantage of the boosted trees is versatility and ease of data interpretation.

Using the Mean Absolute Percent Error (MAPE) formula, the prediction error is calculated as follows:

$$MAPE = 100\% \cdot \frac{1}{n} \sum_{i=1}^n \frac{|y_{i(true)} - y_{i(prediction)}|}{|y_{i(true)}|}, \quad (4)$$

where  $y_{i(prediction)}$  is the predicted element of the sample;  $y_{i(true)}$  is the real value of the element of the sample;  $n$  is the size of the study sample.

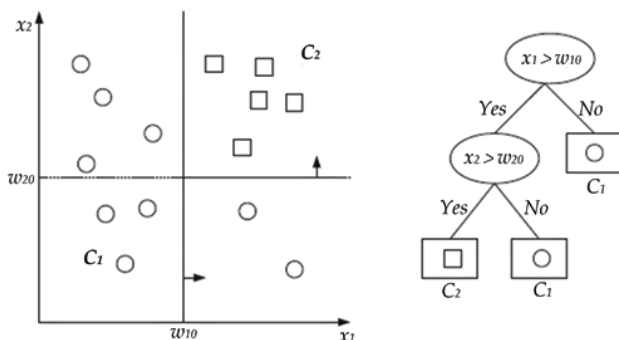


**Figure 2.** Example of a data set and the corresponding decision tree (Alpayndin, 2010)

### 3. Results and discussion

#### 3.1. Composition of the filled epoxy polymers reinforced with basalt and glass fiber

The introduction of fillers into epoxy composite materials is known to increase the heat resistance of the composites compared to that of the polymer binder. Accordingly, the heat resistance of epoxy composites depends both on the filler's nature and the specifics of the particle surface. In particular, the presence of active ( $\gamma$ -aminopropyl-aerosil and aerosil) and inert ( $Al_2O_3$  and  $Cr_2O_3$ ) fillers allows increasing the thermal stability limits of epoxy composites. Therefore, the introduction of fillers that are chemically active in relation to the matrix provides for a more significant effect, which manifests itself in increasing the temperature of thermal fracture of the filled polymer materials compared to  $Al_2O_3$  and  $Cr_2O_3$ . In the formation of epoxy CMs, the ED-20 epoxy dian oligomer (GOST 10587-84) was chosen as the main binding component characterized by high adhesive and cohesive strength, low shrinkage and high manufacturability during application.

Polyethylene polyamine PEPA hardener (TU 6-05-241-202-78) was used for crosslinking epoxy compositions, making it possible for the materials to harden at room temperatures. PEPA is known (Dobrotvor et al., 2021) to be a low molecular weight substance with the following chemical formula:  $[-CH_2-CH_2-NH-]_n$ . CMs were cross-linked by introducing a hardener into the composition at a stoichiometric ratio of components by content (wt %) – ED-20: PEPA – 100: 10. The scheme of the epoxy composite is given in Table 1.

**Table 1.** Composition of the filled epoxy polymers reinforced with basalt and glass fiber

Filler	Concentration, wt %	Reinforcing fibrous filler
Aerosil	2	glass fiber
		basalt fiber
	6	glass fiber
		basalt fiber
	12	glass fiber
		basalt fiber
g-aminopropyl-aerosil	2	glass fiber
		basalt fiber
	6	glass fiber
		basalt fiber
	12	glass fiber
		basalt fiber
$Cr_2O_3$	30	glass fiber
		basalt fiber
	50	glass fiber
		basalt fiber
	100	glass fiber
		basalt fiber
$Al_2O_3$	30	glass fiber
		basalt fiber
	50	glass fiber
		basalt fiber
	100	glass fiber
		basalt fiber

### 3.2. Thermal conductivity coefficients of filled epoxy polymers

To model the dependence of the thermal conductivity coefficient on the mass fraction concentration of the filler and temperature, the mass fraction concentration of the filler and temperature served as input parameters, while the thermal conductivity coefficient  $\lambda$  was considered as an output parameter.

The thermal conductivity coefficient of epoxy polymers reinforced with glass fiber and filled with aerosil,  $\gamma$ -aminopropylaerosil, aluminum oxide, chromium oxide, respectively, was predicted on the basis of the experimental data obtained in Mykytyshyn (2002) by various methods of machine learning, in particular, neural networks and boosted decision trees.

In the process of learning, the data set was divided into two unequal parts – the training sample and the test sample. The sample contained 4,000 elements for each epoxy polymer reinforced with fiberglass and filled with aerosil and  $\gamma$ -aminopropylaerosil, respectively, and 28,000 elements for the polymer filled with aluminum oxide and chromium oxide, respectively, of which 80% were randomly selected for the learning sample, and 20% were left to assess the prediction quality. In particular, to achieve this number of elements, the dataset was expanded using spline interpolation.

To model the dependence of the thermal conductivity coefficient on the mass fraction concentration of the filler and temperature, the thermal conductivity coefficient  $\lambda$  served as an input parameter, while the mass fraction concentration of the filler and temperature were considered as output parameters.

Machine learning methods were used to construct the dependences of the experimental data relating to the thermal conductivity coefficient on the predicted data (Figures 3–6). The prediction results were found to be in good agreement with the experimental ones.

It is noteworthy that points are located close to the bisector of the first coordinate angle in Figures 3–6, indicating a linear relationship between the predicted and experimental data. The NN method gives an error of 0.5% for epoxy composites filled with aerosil and  $\gamma$ -aminopropylaerosil, 0.3% and 0.2% for epoxy composites filled with aluminum oxide and chromium oxide, respectively. At the same time, the error of the boosted decision tree method is 1.5% for epoxy composites filled with aerosil,  $\gamma$ -aminopropylaerosil, and aluminum oxide, respectively, and 0.9% for epoxy composite filled with chromium oxide. Figures 7–10 show the dependence of the predicted thermal conductivity coefficient on the mass fraction concentration of the filler and temperature of the test sample obtained by various methods of machine learning.

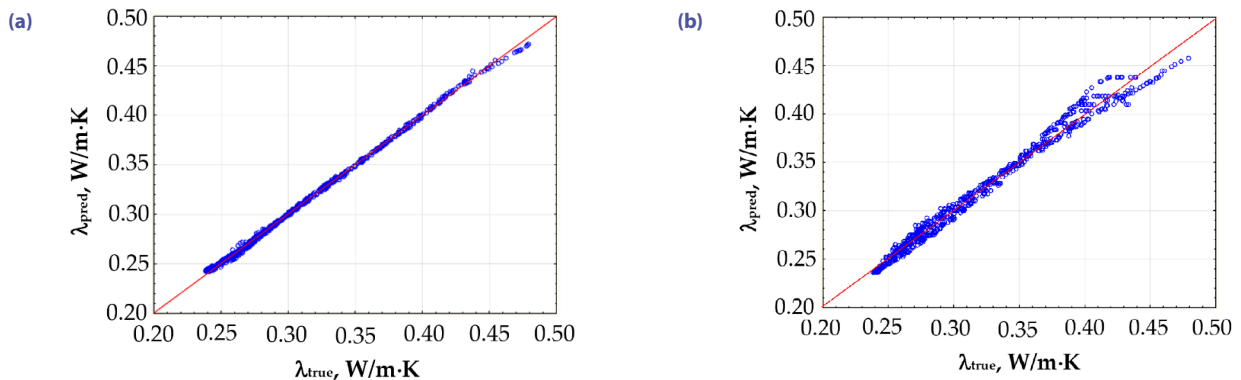


**Figure 3.** Predicted and experimental dependences of the thermal conductivity coefficient for an epoxy composite filled with aerosil obtained by the method of neural networks (a) and boosted decision trees (b)

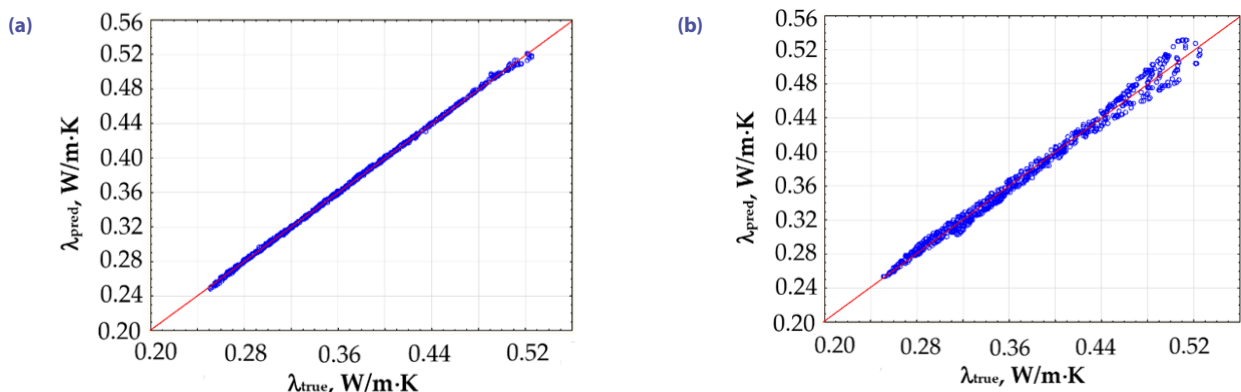


**Figure 4.** Predicted and experimental dependences of the thermal conductivity coefficient for an epoxy composite filled with  $\gamma$ -aminopropylaerosil obtained by the method of neural networks (a) and boosted decision trees (b)

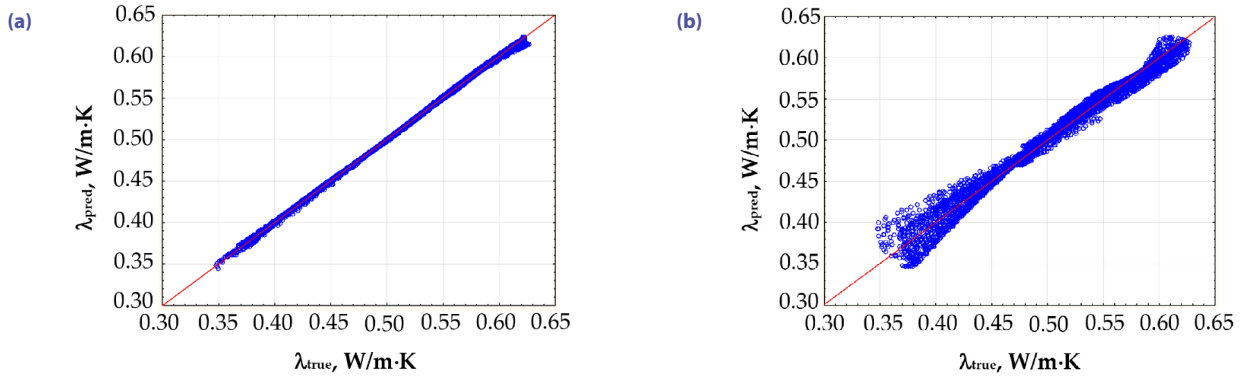


**Figure 5.** Predicted and experimental dependences of the thermal conductivity coefficient for an epoxy composite filled with aluminum oxide obtained by the method of neural networks (a) and boosted decision trees (b)

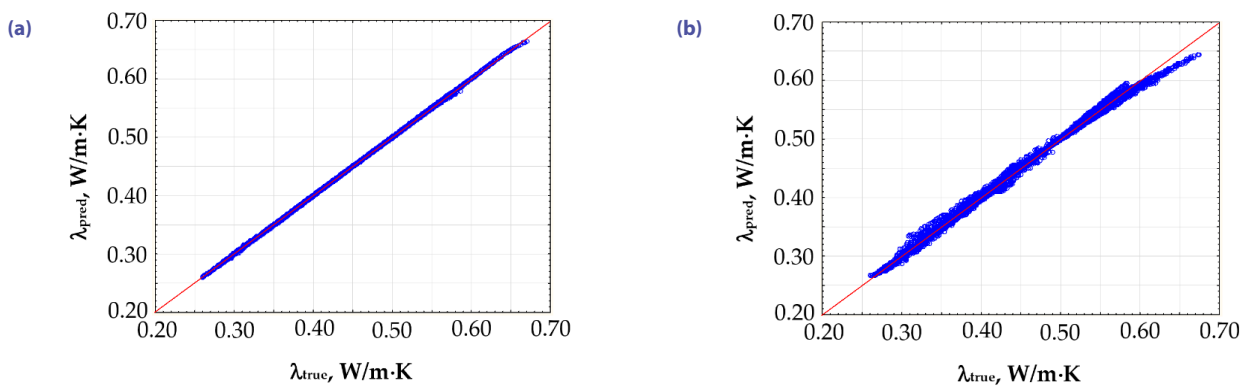


**Figure 6.** Predicted and experimental dependences of the thermal conductivity coefficient for an epoxy composite filled with chromium oxide obtained by the method of neural networks (a) and boosted decision trees (b)

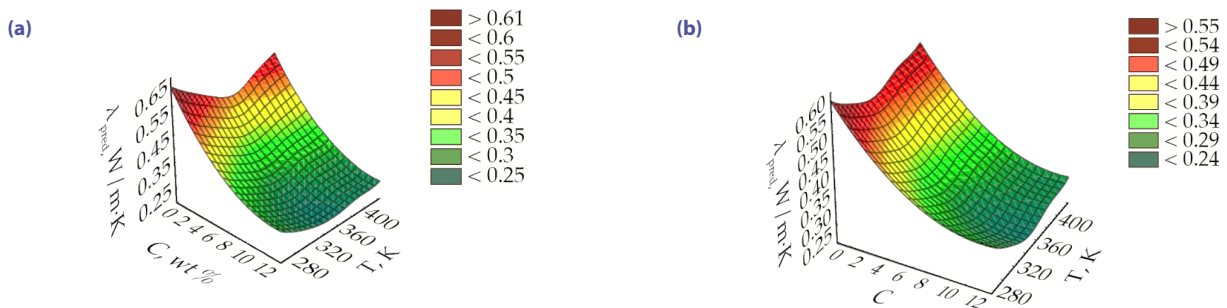


**Figure 7.** Temperature dependence of changes in the thermal conductivity coefficient for the composite filled with aerosil obtained by the method of neural networks (a) and boosted decision trees (b)

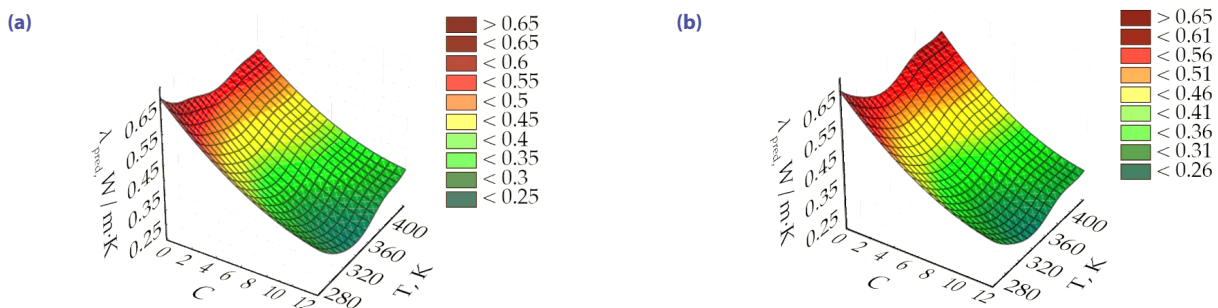


**Figure 8.** Temperature dependence of changes in the thermal conductivity coefficient for the composite filled with  $\gamma$ -aminopropyl-aerosil obtained by the method of neural networks (a) and boosted decision trees (b)



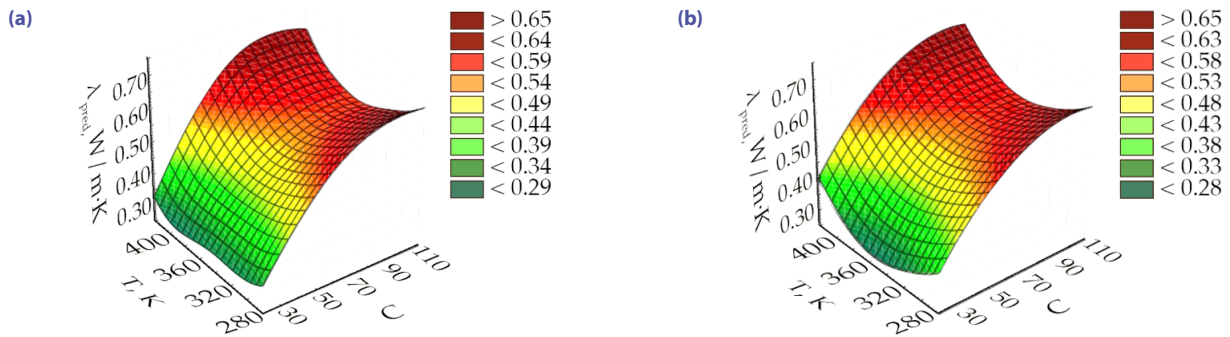


**Figure 9.** Temperature dependence of changes in the thermal conductivity coefficient for the composite filled with aluminum oxide obtained by the method of neural networks (a) and boosted decision trees (b)

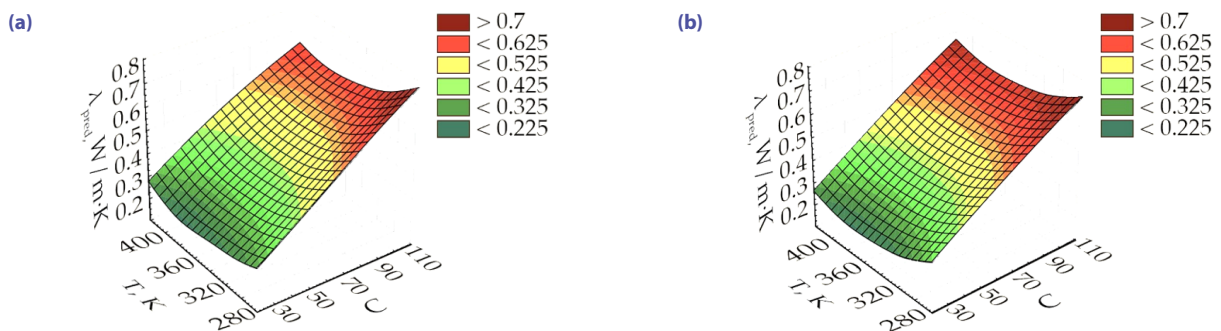


**Figure 10.** Temperature dependence of changes in the thermal conductivity coefficient for the epoxy composite filled with chromium oxide obtained by the method of neural networks (a) and boosted decision trees (b)

The main parameters of machine learning algorithms, in particular, neural networks and boosted decision trees, are given in Table 2–3. The statistical graph used for the data analysis presents as a histogram of residual values, which shows the frequency of each interval of values versus residual values. In particular, the residuals show the difference between the experimental and predicted values.

They were found to be concentrated around zero and have a normal distribution.

Figures 11–14 show frequency for epoxy composites reinforced by glass fiber and filled with Aerosil,  $\gamma$ -aminopropylsilane, aluminum oxide, chromium oxide, respectively, using different machine learning methods, in particular, neural networks and boosted decision trees.

**Table 2.** Parameters of neural networks

Filler	Name of network	Algorithm of learning	Error function	Function of hidden activation	Function of output activation
Aerosil	MLP 2-8-1	BFGS	SOS	Logarithmic	Logarithmic
$\gamma$ -aminopropylsilane	MLP 2-8-1	BFGS	SOS	Logarithmic	Tangential
$\text{Al}_2\text{O}_3$ ; $\text{Cr}_2\text{O}_3$	MLP 2-7-1	BFGS	SOS	Tangential	Tangential

**Table 3.** Parameters of reinforced trees

Filler	Number of trees
Aerosil, $\gamma$ -aminopropylsilane, $\text{Al}_2\text{O}_3$ ; $\text{Cr}_2\text{O}_3$	1000

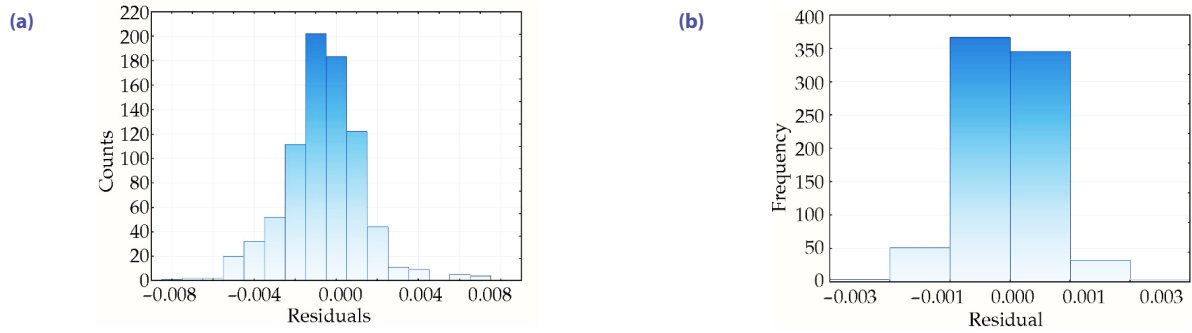


**Figure 11.** Frequency in the test set for the epoxy composite filled with aerosil obtained by the method of neural networks (a) and boosted decision trees (b)

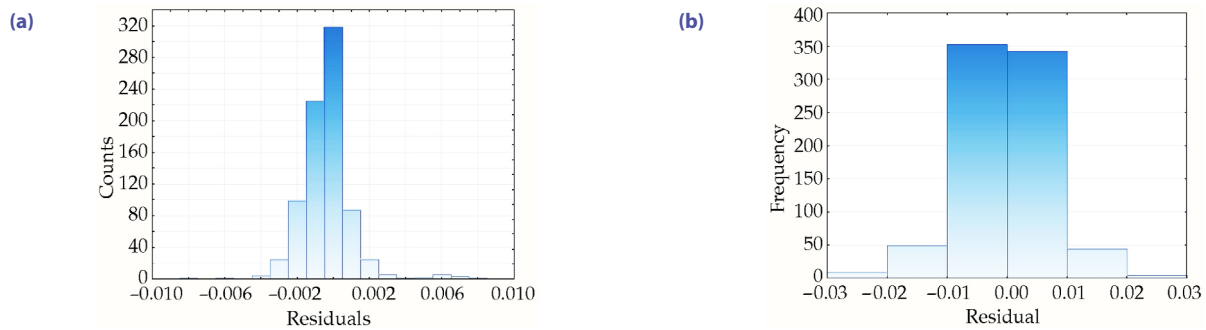


**Figure 12.** Frequency in the test set for the epoxy composite filled with  $\gamma$ -aminopropyl-aerosil obtained by the method of neural networks (a) and boosted decision trees (b)

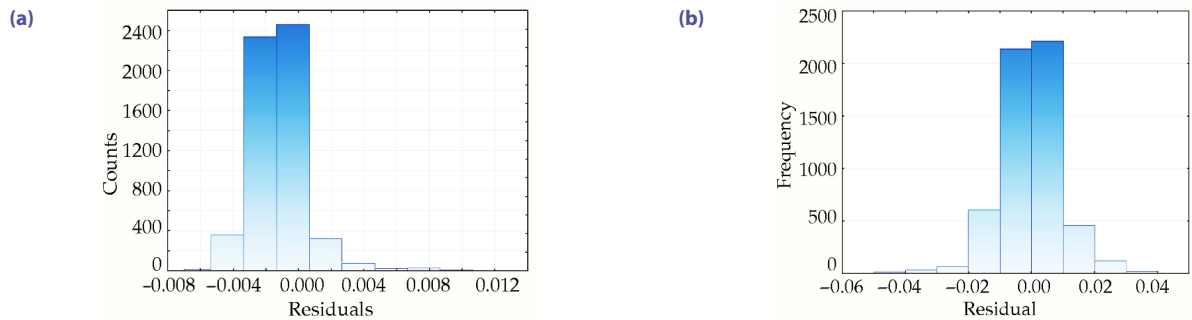


**Figure 13.** Frequency in the test set for the epoxy composite filled with aluminum oxide obtained by the method of neural networks (a) and boosted decision trees (b)

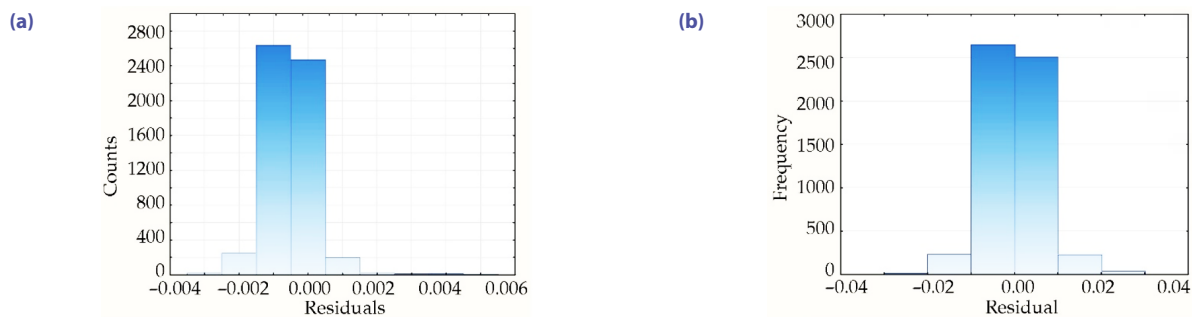


**Figure 14.** Frequency in the test set for the epoxy composite filled with chromium oxide obtained by the method of neural networks (a) and boosted decision trees (b)

## 4. Conclusions

Once predicted, thermal conductivity can provide important information about the thermal properties of a material. It also aids a lot in understanding thermal performance of the material, making it easier to investigate and develop new composites for various applications. In particular, knowing thermal conductivity is crucial in the design of structures and materials, especially composites with different fillers. Materials with improved thermal performance can be created for such industries as civil engineering, aviation, electronics, and so on.

Machine learning methods, such as neural networks and boosted trees, were used to simulate the thermal conductivity coefficient of epoxy polymers reinforced by glass fiber and filled with aerosil,  $\gamma$ -aminopropyl aerosil, aluminum oxide, chromium oxide, respectively. Neural networks had a prediction error of 0.5%, 0.3%, and 0.2% when evaluating different test samples. At the same time, boosted trees had a slightly higher prediction error, which was 1.5% and 0.9%, respectively. Despite these differences, both machine learning methods proved to be efficient at predicting thermal conductivity coefficients. This makes them very promising in materials science. Very low prediction errors further emphasize the accuracy and reliability of these models in the analysis of the complex relationships between the composite materials studied.

## Author contributions

Conceptualization, O. Y. and I. D.; methodology, O. Y. and I. D.; validation, P. M. and A. M.; formal analysis, M. M.; investigation, I. D., O. Y., P. M., A. M., M. M.; data curation, I. D.; writing – original draft preparation, I. D., O. Y., P. M., A. M., M. M.; writing – review and editing I. D.; visualization, O. Y.; supervision, M. M. and A. M.; project administration, P. M. All authors have read and agreed to the published version of the manuscript.

## Disclosure statement

The data are available from the corresponding author upon reasonable requests.

## References

- Alpayndin, E. (2010). Introduction to machine learning. *The Knowledge Engineering Review*, 25(3), 353–353. <https://doi.org/10.101497/S0269888910000056>
- Bezerra, E. M., Ancelotti, A. C., Pardini, L. C., Rocco, J. A. F. F., Iha, K., & Ribeiro, C. H. C. (2007). Artificial neural networks applied to epoxy composites reinforced with carbon and E-glass fibers: Analysis of the shear mechanical properties. *Materials Science and Engineering A*, 464(1–2), 177–185. <https://doi.org/10.1016/j.msea.2007.01.131>
- Dobrotvor, I. G., Stukhlyak, P. D., Mykytyshyn, A. G., & Stukhlyak, D. P. (2021). Influence of thickness and dispersed impurities on residual stresses in epoxy composite coatings. *Strength of Materials*, 53, 283–290. <https://doi.org/10.1007/s11223-021-00287-x>
- Haykin, S. (2006). *Neural networks – a comprehensive foundation*. Prentice Hall.
- Konovalenko, I., Maruschak, P., Brevus, V., & Prentkovskis, O. (2021). Recognition of scratches and abrasions on metal surfaces using a classifier based on a convolutional neural network. *Metals*, 11(4), Article 549. <https://doi.org/10.3390/met11040549>
- Liu, B., Vu-Bac, N., Zhuang, X., Fu, X., & Rabczuk, T. (2022). Stochastic integrated machine learning based multiscale approach for the prediction of the thermal conductivity in carbon nanotube reinforced polymeric composites. *Composites Science and Technology*, 224, Article 109425. <https://doi.org/10.1016/j.compscitech.2022.109425>
- Mohanty, J. R., Verma, B. B., Parhi, D. R. K., & Ray, P. K. (2009). Application of artificial neural network for predicting fatigue crack propagation life of aluminum alloys. *Archives of Computational Materials Science and Surface Engineering*, 1(3), 133–138.
- Monticeli, F. M., Neves, R. M., Ornaghi, H. L., & Almeida, J. H. S. (2022). Prediction of bending properties for 3D-printed carbon fibre/epoxy composites with several processing parameters using ANN and statistical methods. *Polymers*, 14(17), Article 3668. <https://doi.org/10.3390/polym14173668>
- Mykytyshyn, A. G. (2002). *Development of technology and study of parameters of formation of products from epoxy-filled composites*, [Dissertation, Lviv Polytechnic National University]. Lviv (in Ukrainian).
- Stephen, C., Thekkuden, D. T., Mourad, A. H. I., Shivamurthy, B., Selvam, R., & Rohit Behara, S. (2022). Prediction of impact performance of fiber reinforced polymer composites using finite element analysis and artificial neural network. *Journal of the Brazilian Society of Mechanical Sciences and Engineering*, 44, Article 408. <https://doi.org/10.1007/s40430-022-03711-8>
- Stukhlyak, P. D., Buketov, A.V., Panin, S. V., Maruschak, P. O., Moroz, K. M., Poltaranin, M. A., Vukherer, T., Kornienko, L. A., & Lyukshin, B. A. (2015). Structural fracture scales in shock-loaded epoxy composites. *Physical Mesomechanics*, 18, 58–74. <https://doi.org/10.1134/S1029959915010075>
- Yasnii, O. P., Pastukh, O. A., Pyndus, Y. I., Lutsyk, N. S., & Didych I. S. (2018). Prediction of the diagrams of fatigue fracture of D16T aluminum alloy by the methods of machine learning. *Materials Science*, 54, 333–338. <https://doi.org/10.1007/s11003-018-0189-9>
- Yasniy, O., Didych, I., Fedak, S., & Lapusta, Y. (2020). Modeling of AMg6 aluminum alloy jump-like deformation properties by machine learning methods. *Procedia Structural Integrity*, 28, 1392–1398. <https://doi.org/10.1016/j.prostr.2020.10.110>
- Yasniy, O., Fedak, S., & Lapusta, Y. (2022a). Prediction of jump-like creep using preliminary plastic strain. *Procedia Structural Integrity*, 36, 166–170. <https://doi.org/10.1016/j.prostr.2022.01.019>
- Yasniy, O., Pasternak, I., & Sobashek, L. (2022b). Modelling of AL-6061 aluminum alloy deformation diagrams by machine learning methods. *Procedia Structural Integrity*, 42, 1344–1349. <https://doi.org/10.1016/j.prostr.2022.12.171>
- Zhang, L., & Wei, X. (2022) Prediction of fatigue crack growth under variable amplitude loading by artificial neural network-based Lagrange interpolation. *Mechanics of Materials*, 171, Article 104309. <https://doi.org/10.1016/j.mechmat.2022.104309>